JOURNAL OF PHYSICAL ORGANIC CHEMISTRY
J. Phys. Org. Chem. 2004; **17:** 241–248
Published online in Wiley InterScience (www.interscience.wiley.com). DOI: 10.1002/poc.722

The gas-phase reactivity of epichlorohydrin with hydroxide

G. N. Merrill*

2155 29th Avenue, San Francisco, California 94116, USA

Received 21 August 2003; revised 5 October 2003; accepted 6 October 2003

ABSTRACT: The reaction of hydroxide with epichlorohydrin in the gas phase was investigated with *ab initio* calculations. Three mechanisms were examined, each corresponding to nucleophilic attack at a different carbon atom of the substrate. It was determined that through attack at the ring methylene position was favored, whereas attacks at the alkyl methylene or ring methine positions were found to have larger activation energies. These results are consistent with experimental results found in the literature. Copyright © 2004 John Wiley & Sons, Ltd.

KEYWORDS: epichlorohydrin; hydroxide; reaction mechanism; *ab initio* modeling

INTRODUCTION

Epichlorohydrin is a commercially important compound used in the industrial production of glycerol, resins and elastomers.[1a] It is also a toxic substance, a vesicant and is potentially carcinogenic in humans (see toxicological references in Ref. 1a). Epichlorohydrin has also been used in the synthesis of optical isomers of antihypertensive and antianginal drugs.[1b] For these reasons, epichlorohydrin has been the subject of numerous experimental investigations.

These studies have frequently sought to establish the reaction mechanism between epihalohydrins and nucleophiles. For instance, does the initial attack by the nucleophile occur at the C1 (ring methylene) or C3 (alkyl methylene) position? In the most important examination of the reaction mechanism, McClure *et al.*[2] demonstrated that the answer to this question depends on the choice of leaving group, nucleophile and reaction conditions. Subsequent studies by Ohishi and Nakanishi[3] on epichlorohydrin and by Cawley and Onat[4] on epibromohydrin confirmed that both pathways are active. It should be noted that, with the exception of an acetolysis investigation by Whalen,[5] little attention has been given to the possibility of nucleophilic attack at the C2 (ring methine) position.

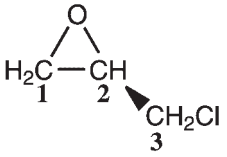

**Correspondence to:* G. N. Merrill, 2155 29th Avenue, San Francisco, California 94116, USA.
E-mail: grant.merrill@comcast.net

In the course of my work with epichlorohydrin as a polymeric cross-linking agent, the question of its reactivity again arose; unexpected products could not be entirely explained by an appeal to the experimental literature. It also appears that no systematic theoretical investigation of the reactivity of epichlorohydrin has been reported. A computational study of limited scope, which included an examination of the reaction of ammonia with epichlorohydrin, has been reported previously[6]. An *ab initio* study into the inherent (gas-phase) reactivity of epichlorohydrin with hydroxide was therefore carried out. While solvation effects will clearly have a strong influence on the current system, the gas-phase reaction coordinates established here will serve as the first step towards a more thorough theoretical understanding of the reactivity of epichlorohydrin in solution under basic conditions.

COMPUTATIONAL METHODS

All structures were fully optimized at the restricted Hartree–Fock (RHF) level of theory with the double split-valence 6–31G basis set of Pople and co-workers[7] to which sets of d-polarization[8] and sp-diffuse[9] functions were added to all non-hydrogen atoms (6–31 + G*). The structures were deemed converged when the maximum and r.m.s. gradients fell below 0.012 and 0.004 kcal $mol^{-1}Å^{-1}$, respectively (1 kcal = 4.184 kJ). Hessian matrices were computed for all stationary points at the same level of theory. The absence of negative eigenvalues confirmed the stationary points as minima, while a single negative eigenvalue defined a stationary point as a transition state. All vibrational frequencies were scaled by a factor of 0.8953 to compensate for the known

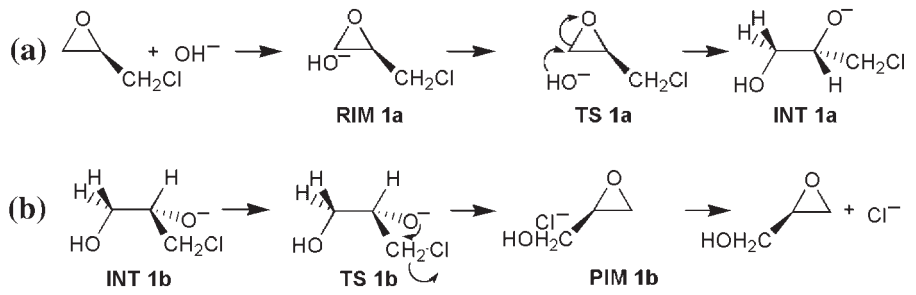

Scheme 1

overestimation of harmonic vibrational frequencies at the Hartree–Fock level with double-zeta quality basis sets.[10] Enthalpies and entropies were computed at 298.15 K and 1 atm using standard equations from statistical mechanics.[11]

Minimum energy paths were determined by carrying out intrinsic reaction coordinate (IRC)[12] calculations from the transition states to the associated 'reactant' and 'product' minima. All minima were subsequently fully optimized and their Hessian matrices computed.

Single-point energy calculations were performed upon all HF stationary structures using second-order Møller–Plesset (MP2)[13] perturbation theory with the augmented, correlation-consistent, double split-valence basis set of Dunning and co-workers (aug-cc-pVDZ).[14] Only the valence electrons were correlated in these calculations, i.e. the frozen core (fc) approximation was used.[15] These calculations were intended to recover the effects of dynamic electron correlation, which can be important in the description of transition states in which bonds are formed or broken.

Finally, all stationary point structures (minima and transition states) were reoptimized at the MP2(fc)/6–31 + G* level of theory. These calculations were performed to assess the importance of dynamic electron correlation on the optimized structures. Enthalpic and entropic corrections were calculated at the HF/6–31 + G* level.

All calculations were carried out with the GAMESS[16] program, which is freely available from Iowa State University, on a cluster of personal computers running the Linux operating system.

RESULTS

Three mechanisms were investigated, each corresponding to nucleophilic attack by hydroxide at a different carbon atom of epichlorohydrin. While a number of elimination pathways involving hydroxide and epichlorohydrin are possible, they were not the focus of this study. The following free energies were calculated at the MP2/aug-cc-pVDZ//HF/6–31 + G* level of theory:

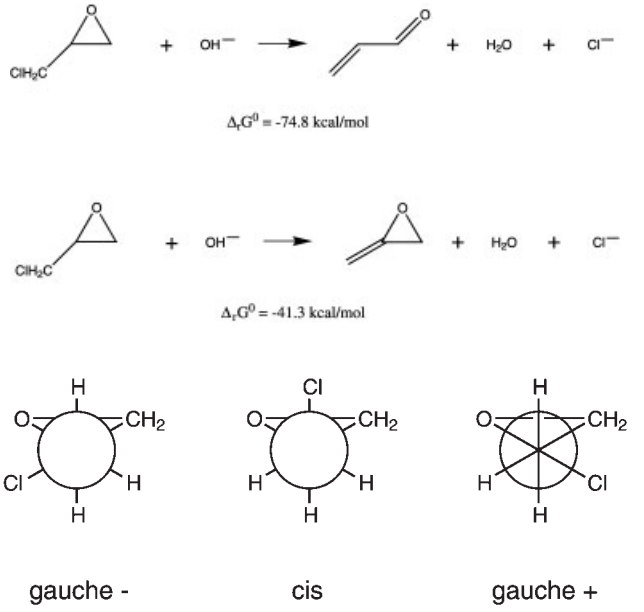

In the first mechanism, nucleophilic attack occurs at the C1 (ring methylene) position, resulting in an oxide intermediate [Scheme 1(a)]. The anionic oxygen atom can then attack the C3 (alkyl methylene) position to form glycidol with the loss of chloride [Scheme 1(b)]. Both reactant ion–molecule (RIM) and product ion–molecule (PIM) complexes are formed along the gas-phase pathway; the reactant complex is composed of hydroxide and epichlorohydrin, and the product complex is formed from chloride and glycidol. As three minimum-energy conformers exist for epichlorohydrin (*gauche*−, *cis* and *gauche*+) [at the MP2 level of theory, the relative free energies of the three conformers are *cis* (1.5 kcal mol^{-1}) > *gauche*− (0.4 kcal mol^{-1}) > gauche+ (0.0 kcal mol^{-1}); this translates into a Boltzmann population of *cis* (5%) < gauche− (32%) < gauche+ (63%); these results reproduce those found in the literature at the B3LYP/6–311G(2d,2p) level of theory[17]], there are also three possible transition states (TS) for the C1 mechanism. All three transition states were located at the Hartree–Fock (HF) level of theory.

In the second mechanism, nucleophilic attack takes place at the C2 (ring methine) position, which results in ring opening of the epoxide to form an oxide intermediate

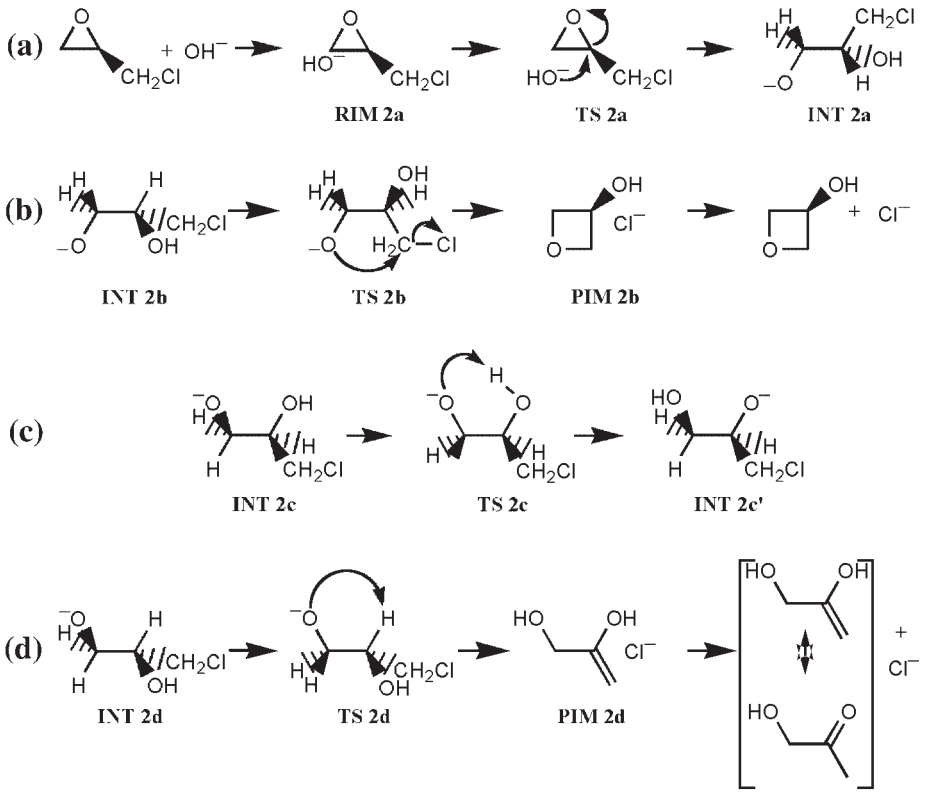

Scheme 2

(Scheme 2a). A reactant (hydroxide–epichlorohydrin) ion–molecule complex was again found, and numerous attempts to locate three transition states led only to the two *gauche*-related structures. Upon formation of the oxide intermediate, three subsequent reaction steps were investigated: (1) attack by the anionic oxygen atom on the C3 (alkyl methylene) position to yield 2-hydroxyoxetane with loss of chloride [Scheme 2(b)]; two transition states and product (chloride–oxetane) ion–molecule complexes were located for this pathway; (2) proton transfer between the hydroxyl group and the anionic oxygen atom to produce another oxide intermediate [Scheme 2(c)], followed by the attack of the new anionic oxygen atom on the C3 (alkyl methylene) position to form glycidol with loss of chloride [Scheme 1(b)]; three transition states and product (chloride–glycidol) ion–molecule complexes were found; (3) proton transfer from the C2 methine position to the anionic oxygen atom accompanied by the elimination of chloride to form a 2-propen-1,3-diol [Scheme 2(d)]; two transition states and product (chloride–diol) ion–molecule complexes were located.

For the third mechanism studied, nucleophilic attack occurs at the C3 (alkyl methylene) position, resulting in the direct displacement of chloride to form glycidol (Scheme 3). Only two transition states, associated with the *gauche* conformers, reactant (hydroxide–epichlorohydrin), and product (chloride–glycidol) ion–molecule complexes were found.

It should be noted that the complete reaction coordinates for the C1 and C2 pathways are not given in Schemes 1 and 2, respectively. The missing steps correspond to low-energy transitions between conformers (e.g. **INT 1a** → **INT 1b** in Scheme 1). As they are not predicted to be rate-limiting steps, they are not discussed.

The reaction path energetics for Schemes 1–3 are given in Tables 1–3, respectively. For the sake of clarity, only results from the lowest energy pathways are given. Both enthalpies ($\Delta_r H°$) and free energies ($\Delta_r G°$) at 298.15 K and 1 atm are provided at the Hartree–Fock (HF) and Møller–Plesset (MP2) levels of theory. The structures corresponding to important stationary points are presented in Figs 1–3.

A known deficiency of Hartree–Fock theory is the overestimation of activation energies (E_a).[18] This is particularly true for transition states in which bonds are formed or broken. In these transition states, dynamic

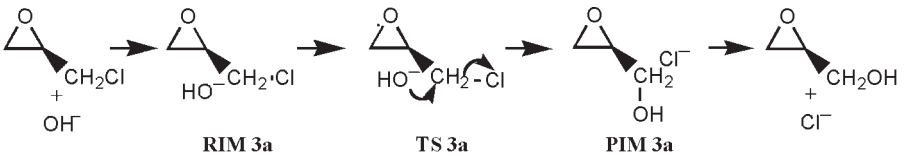

Scheme 3

Table 1. Reaction coordinate energetics for nucleophilic attack on the C1 position of epichlorohydrin [Scheme 1(a) and 1(b)][a]

Level of theory	Epichlorohydrin + hydroxide	Reactant ion–molecule (**RIM 1a**)	Transition state (**TS 1a**)	Intermediate (**INT 1a**)
	$\Delta_r H^\circ$ [Scheme 1(a): attack on C1 position]			
HF	0.0	−21.5	−7.1 (599 i cm^{-1})	−50.9
MP2	0.0	−23.8	−16.6	−48.1
	$\Delta_r G^\circ$ [Scheme 1(a): attack on C1 position]			
HF	0.0	−14.1	1.6	−41.4
MP2	0.0	−16.4	−7.9	−38.6
	$\Delta_r H^\circ$ [Scheme 1(b): epoxide formation]			
	Intermediate (**INT 1b**)	Transition state (**TS 1b**)	Product ion–molecule (**PIM 1b**)	Glycidol + chloride
HF	−61.3	−53.9 (418 i cm^{-1})	−79.1	−69.9
MP2	−59.8	−51.7	−62.4	−50.3
	$\Delta_r G^\circ$ [Scheme 1(b): epoxide formation]			
HF	−51.3	−43.9	−71.7	−67.8
MP2	−49.7	−41.8	−55.0	−48.2

[a] Standard enthalpies ($\Delta_r H^\circ$) and free energies ($\Delta_r G^\circ$) in kcal mol^{-1}. Parenthetical values correspond to transition-state imaginary vibrational frequencies. HF = HF/6–31 + G*; MP2 = MP2/aug-cc-pVDZ//HF/6–31 + G*. See text for details.

electron correlation effects can be large. It is not surprising, therefore, that HF theory, which takes no account of dynamic electron correlation, fails to describe the present transition states adequately. Results obtained at the Møller–Plesset level of theory will, therefore, be focused upon in the Discussion.

A comparison of the results predicated upon HF and MP2 optimized structures reveals that dynamic electron correlation does not have a significant effect on the structures and thus energetics. [The following enthalpies and free energies of activation, based upon MP2(fc)/6–31 + G* optimizations and HF/6–31 + G* Hessians, were calculated: $\Delta_r H^\circ$(**TS1a**) = −15.2; $\Delta_r H^\circ$(**TS2a**) = −12.1; $\Delta_r H^\circ$(**TS3a**) = −14.0; $\Delta_r G^\circ$ (**TS1a**) = −6.5; $\Delta_r G^\circ$ (**TS2a**) = −3.1; and $\Delta_r G^\circ$(**TS3a**) = −5.3 kcal mol^{-1}. These values compare very favorable with those obtained at the highest level of theory reported in this paper: MP2(fc)/aug-cc-pVDZ//HF/6–31 + G* (Tables 1–3). Examining the HF and MP2 structures for these transition states also reveals that the two sets of structures are in good agreement with one another. Comparing the distances associated with the reaction coordinates for the three transition states evinces a mean difference and standard deviation of only −0.01 and 0.05 Å, respectively.] This validation of the current computational approach (MP2 single-point energies on HF optimized structures) is important for reasons beyond the current study. First, an investigation into the effects of solvation upon the reactivity of epichlorohydrin under basic conditions is currently being conducted. The approach undertaken in this work is one of microsolvation, where the solutes are surrounded with a number of solvent molecules. Optimizations at the MP2 level would, therefore, prove very costly in this context. Second, these results underscore the importance of selecting the appropriate level of theory. Too often computational chemistry is marginalized by the demand that only the highest level of theory be employed. This attitude severely limits the applicability of *ab initio* methods.

DISCUSSION

A cursory examination of the energetics for the three mechanisms reveals that initial nucleophilic attack on the substrate is the rate-limiting step. Based on previous studies of ambident substrates, it is predicted that the S_N2 mechanism should be favored under basic conditions. Nucleophilic attack should, therefore, take place at the least substituted position, i.e. C3 > C1 > C2. Attack at the ring methylene (C1) position [Scheme 1(a)] has a lower activation energy than attack at the alkyl methylene (C3) position (Scheme 3), while attack at the C2 methine position [Scheme 2(a)] possesses the largest activation energy. The relative activation enthalpies are 3.1 (C2) > 1.6 (C3) > 0.0 (C1) kcal mol^{-1}. The relative activation free energies similarly are 3.3 (C2) > 1.6 (C3) > 0.0 (C1) kcal mol^{-1}. The inclusion of entropic effects serves, therefore, only to raise the absolute activation energies for the three transition states. The associated imaginary frequencies for the C1, C2 and C3 transition states are 599, 610 and 418 cm^{-1}, respectively, revealing that the C1 and C2 transition states are tighter and less accessible than the C3 transition state. This should in turn favor nucleophilic

Table 2. Reaction coordinate energetics for nucleophilic attack on the C2 position of epichlorohydrin [Schemes 2(a)–(d)][a]

Level of theory	Epichlorohydrin + hydroxide	Reactant ion–molecule (**RIM 2a**)	Transition state (**TS 2a**)	Intermediate (**INT 2a**)
	$\Delta_r H^\circ$ [Scheme 2(a): attack on C2 position]			
HF	0.0	−21.5	−1.9 (610 i cm^{-1})	−50.8
MP2	0.0	−23.8	−13.5	−48.1
	$\Delta_r G^\circ$ [Scheme 2(a): attack on C2 position]			
HF	0.0	−15.0	7.0	−41.3
MP2	0.0	−17.3	−4.6	−38.7

Level of theory	Intermediate (**INT 2b**)	Transition state (**TS 2b**)	Product ion–molecule (**PIM 2b**)	2-Hydroxyoxetane + chloride
	$\Delta_r H^\circ$ [Scheme 2(b): oxetane formation]			
HF	−50.5	−42.1 (455 i cm^{-1})	−113.8	−70.9
MP2	−47.2	−38.5	−70.9	−49.6
	$\Delta_r G^\circ$ [Scheme 2(b): oxetane formation]			
HF	−40.7	−31.8	−105.8	−68.7
MP2	−37.5	−28.2	−62.8	−47.3

Level of theory	Intermediate (**INT 2c**)	Transition state (**TS 2c**)	Intermediate (**INT 2c′**)
	$\Delta_r H^\circ$ [Scheme 2(c): proton transfer from C2 hydroxyl to C3 oxide]		
HF	−56.4	−53.9 (1384 i cm^{-1})	−61.3
MP2	−55.5	−59.5	−59.8
	$\Delta_r G^\circ$ [Scheme 2(c): proton transfer from C2 hydroxyl to C3 oxide]		
HF	−46.3	−43.5	−51.3
MP2	−45.4	−49.1	−49.7

Level of theory	Intermediate (**INT 2d**)	Transition state (**TS 2d**)	Intermediate (**PIM 2d**)	2-Propene-1,3-diol + chloride
	$\Delta_r H^\circ$ [Scheme 2(d): proton transfer from C2 methine to C3 oxide]			
HF	−50.8	4.1 (1925 i cm^{-1})	−102.3	−22.6
MP2	−48.1	−10.6	−89.7	−4.4
	$\Delta_r G^\circ$ [Scheme 2(d): proton transfer from C2 methine to C3 oxide]			
HF	−41.3	13.7	−94.4	−52.8
MP2	−38.7	−1.0	−81.8	−34.6

[a] Standard enthalpies ($\Delta_r H^\circ$) and free energies ($\Delta_r G^\circ$) in kcal mol^{-1}. Parenthetical values correspond to transition-state imaginary vibrational frequencies. HF = HF/6–31 + G*; MP2 = MP2/aug-cc-pVDZ//HF/6–31 + G*. See text for details.

Table 3. Reaction coordinate energetics for nucleophilic attack on the C3 position of epichlorohydrin [Scheme 3][a]

Level of theory	Epichlorohydrin + hydroxide	Reactant ion–molecule (**RIM 3a**)	Transition state (**TS 3a**)	Product ion–molecule (**PIM 3a**)	Glycidol + chloride
	$\Delta_r H^\circ$ [Scheme 3: attack on C3 position]				
HF	0.0	−21.5	−13.7 (418 i cm^{-1})	−79.1	−69.9
MP2	0.0	−23.8	−15.0	−62.4	−50.3
	$\Delta_r G^\circ$ [Scheme 3: attack on C3 position]				
HF	0.0	−14.1	−4.9	−71.7	−67.8
MP2	0.0	−16.4	−6.3	−55.0	−48.2

[a] Standard enthalpies ($\Delta_r H^\circ$) and free energies ($\Delta_r G^\circ$) in kcal mol^{-1}. Parenthetical values correspond to transition state imaginary vibrational frequencies. HF = HF/6–31 + G*; MP2 = MP2/aug-cc-pVDZ//HF/6–31 + G*. See text for details.

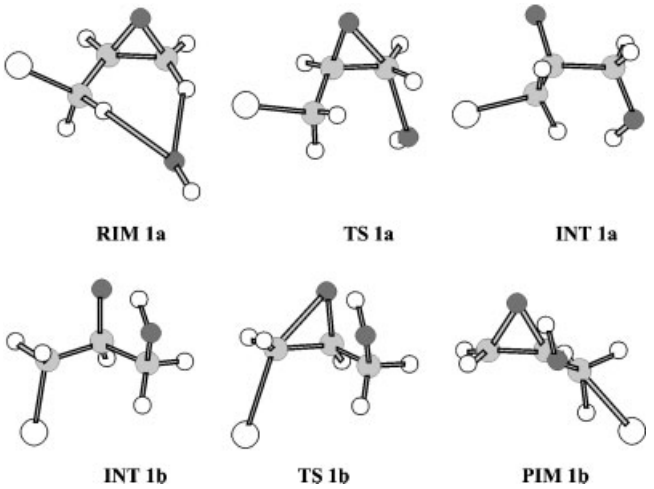

Figure 1. Structures of stationary points along reaction coordinate [Scheme 1(a) and 1(b)] for hydroxide attack at the C1 position of epichlorohydrin. **RIM**, reactant ion–molecule complex; **TS**, transition state; **INT**, intermediate; **PIM**, product ion–molecule complex. See text for details

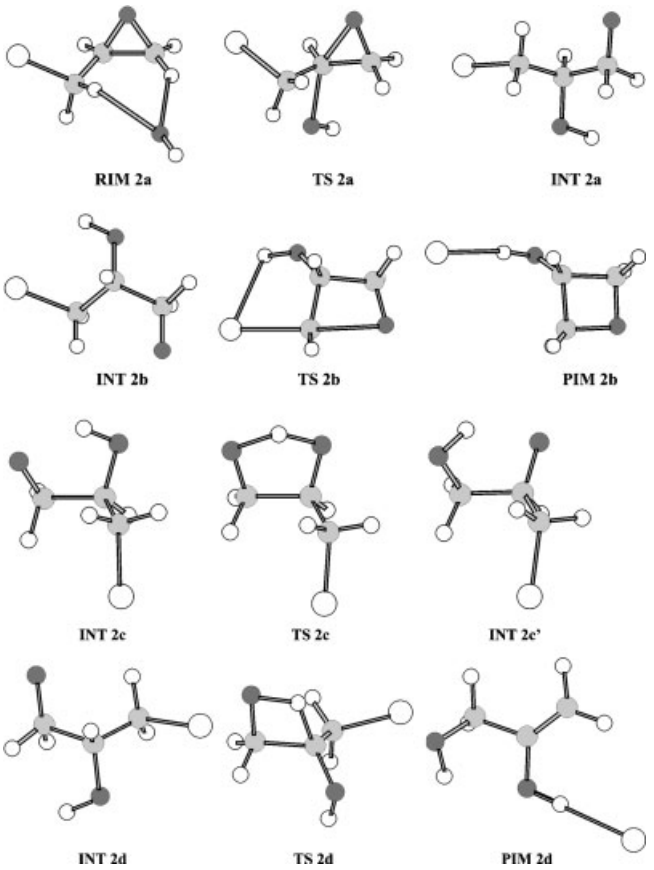

Figure 2. Structures of stationary points along reaction coordinate [Schemes 2(a)–(d)] for hydroxide attack at the C2 position of epichlorohydrin. **RIM**, reactant ion–molecule complex; **TS**, transition state; **INT**, intermediate; **PIM**, product ion–molecule complex. See text for details

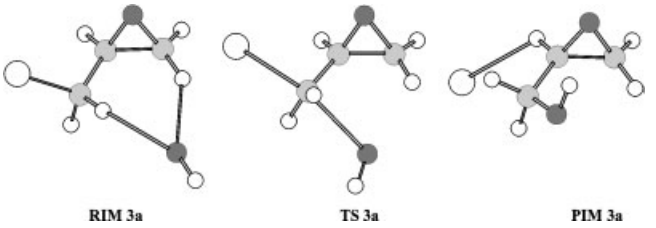

Figure 3. Structures of stationary points along reaction coordinate (Scheme 3) for hydroxide attack at the C3 position of epichlorohydrin. **RIM**, reactant ion–molecule complex; **TS**, transition state; **PIM**, product ion–molecule complex. See text for details

attack at the alkyl methylene position. Based on the activation energies, however, nucleophilic attack should occur at the C1 position resulting in the formation of an oxide intermediate, with attack at the C3 position being less competitive. Assuming a Boltzmann distribution for the activation energies, 93.4% of the reactions should proceed via the C1 pathway and only 6.3% through the C3 pathway. Given the even larger activation energies for the C2 pathway, this mechanism should only be active to a very limited extent (0.4% of the reactions).

These conclusions are fairly consistent with experimental results. Ohishi and Nakanishi[3] reacted a phenolate with radiolabeled epichlorohydrin and discovered that attack at the C1 (ring methylene) position is slightly more favorable than at the C3 (alkyl methylene) position by a 7:5 ratio. No attack was detected at the C2 (ring methine) position. Similarly, Cawley and Onat[4] reacted catecholate anion with epibromohydrin and determined the free energy of activation to be marginally lower for attack at the C1 position: $\Delta_r G^\circ(\mathbf{TS1a}) = 22$ and $\Delta_r G^\circ(\mathbf{TS3a}) = 24\ \text{kcal mol}^{-1}$. As the authors note, while the enthalpic contribution to the free energy of activation is lower for attack at the ring methylene position [$\Delta_r H^\circ(\mathbf{TS1a}) = 12$ and $\Delta_r H^\circ(\mathbf{TS3a}) = 19\ \text{kcal mol}^{-1}$], the entropic contribution is nearly double that for attack at the alkyl methylene position [$\Delta_r S^\circ(\mathbf{TS1a}) = -34$ and $\Delta_r S^\circ(\mathbf{TS3a}) = -18\ \text{cal mol}^{-1}\text{K}^{-1}$]. There is, therefore, a subtle interplay between enthalpy and entropy for this system that slightly favors attack at the C1 position. Again, no attack at the ring methine position was found. This balance between pathways was most dramatically shown by McClure *et al.*[2] when they reacted a number of *para*-substituted phenols with enantiomerically pure epichlorohydrins under a variety of reaction conditions. By examining the products for retention or inversion of configuration, they found that the choice of nucleophile, solvent system and reaction conditions determined whether attack occurred at the C1 or C3 position.

It must be noted that the HF level of theory predicts a different ordering of the transition states for this initial step: C2 > C1 > C3. The relative differences in activation energies are also greater. Both the enthalpies and free energies for attack at the ring methylene position are four times larger than for attack at the alkyl methylene

position. Similarly, the enthalpies and free energies for the C2 transition state are nearly four times larger at the HF level than at the MP2 level. Effectively 100% of the reactions should proceed through the C3 transition state. The exclusion of dynamic electron correlation, therefore, favors the C3 pathway over the C1 pathway. This result stands in contrast with experimental results.[2–4]

Nucleophilic attack at the ring methylene position opens the epoxide to form an oxide intermediate. A new epoxide can be formed via attack of the anionic oxygen atom on the alkyl methylene position with loss of chloride [Scheme 1(b)]. The activation energies for this process are significantly lower than those for the initial nucleophilic attack [$E_a(H^\circ) = -35.1$ and $E_a(G^\circ) = -33.9\,\text{kcal mol}^{-1}$]. Examination of the associated imaginary frequency ($418\,\text{cm}^{-1}$) reveals that this transition state is also less demanding than for the initial attack. Consequently, glycidol should be readily formed by attack at both C1 and C3 positions.

As stated in the Results section, nucleophilic attack at the ring methine position may be followed by three different steps. Both the transition states for oxetane formation [Scheme 2(b)] and proton transfer from the hydroxyl group [Scheme 2(c)] are lower in energy than that for initial attack. Proton transfer is favored over oxetane formation [$\Delta E_a(H^\circ) = -21.0$ and $\Delta E_a(G^\circ) = -20.9\,\text{kcal mol}^{-1}$). The imaginary vibrational frequency for oxetane formation ($455\,\text{cm}^{-1}$) is far smaller than for proton transfer ($1384\,\text{cm}^{-1}$) and should favor oxetane formation. An elimination pathway involving proton transfer from the methine group to form the diol [Scheme 2(d)] was also investigated. An activation energy larger than for the initial attack was found [$\Delta E_a(H^\circ) = 2.9$ and $\Delta E_a(G^\circ) = 3.6\,\text{kcal mol}^{-1}$). The associated imaginary vibrational frequency is $1925\,\text{cm}^{-1}$. Based on these results, it is predicted that nucleophilic attack at the C2 position should lead to glycidol formation (via proton transfer from the hydroxyl group to the anionic oxygen atom followed by epoxide formation). Oxetane should be a minor product to the extent that it is formed at all, and diol formation should not occur.

The formation of glycidol (Schemes 1–3) and oxetane (Scheme 2) are exothermic (glycidol pathways: $\Delta_r H^\circ = -50.3$ and $\Delta_r G^\circ = -48.2\,\text{kcal mol}^{-1}$; oxetane pathways: $\Delta_r H^\circ = -49.6$ and $\Delta_r G^\circ = -47.3\,\text{kcal mol}^{-1}$). Given these small differences in exothermicities, the product distribution for the reaction of hydroxide with epichlorohydrin should be under kinetic control. While the formation of the diol is also thermodynamically favorable ($\Delta_r H^\circ = -4.4\,\text{kcal/mol}$ and $\Delta_r G^\circ = -34.6\,\text{kcal mol}^{-1}$), the associated activation energies are greater than those for the formation of glycidol or oxetane.

Both glycidol and 2-hydroxyoxetane are subject to further nucleophilic attack. These reactions were not investigated, but as basic conditions favor S_N2 mechanisms, attack would presumably occur at the least substituted positions and should be thermodynamically favored. Both steps are indeed exothermic. Using experimental heats of formation for water ($\Delta_f H^\circ = -57.8\,\text{kcal mol}^{-1}$) and glycerol ($\Delta_f H^\circ = -138.1\,\text{kcal mol}^{-1}$), and using Benson's group equivalent scheme to calculate the heats of formation for glycidol ($\Delta_f H^\circ = -58.0\,\text{kcal mol}^{-1}$) and 2-hydroxyoxetane ($\Delta_f H^\circ = -59.2\,\text{kcal mol}^{-1}$), the following reaction enthalpies were computed:

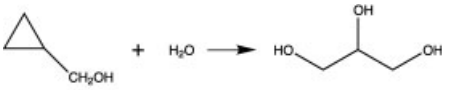

$\Delta_r H^0 = -22.3$ kcal/mol

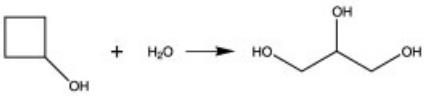

$\Delta_r H^0 = -21.1$ kcal/mol

[$\Delta_f H^\circ(H_2O)$, Ref. 19; $\Delta_f H^\circ(C_3H_8O_3)$, Ref. 20; group equivalents, Ref. 21].

It is reasonable to wonder if the intermediate oxides formed in Schemes 1 and 2 could abstract a proton from an aqueous solvent system and thus preclude glycidol or oxetane formation. While solvent effects were not explicitly considered in the current work, such a process is unlikely in the gas phase. The oxides should be significantly less basis than hydroxide, and their conjugate acids should not form to any great extent. [The conjugate acids of the oxides can be modeled by 1,2-dihydroxyethane (ethylene glycol). Its gas-phase acidity has been measured: $\Delta_r G^\circ = 360.9 \pm 2.0\,\text{kcal mol}^{-1}$.[22] Likewise, the gas-phase acidity of water is experimentally known: $\Delta_r G^\circ = 383.7 \pm 0.3\,\text{kcal mol}^{-1}$.[23] The transfer of a proton from water to the oxides of ethylene glycol is appreciably endothermic and should not occur in the gas phase. The pK_a for ethylene glycol is not known conclusively.] A comparison of the pK_as would be more meaningful, but experimental values for the oxides in question are not known.

$\Delta_r G^0 = +22.8$ kcal/mol

CONCLUSIONS

The reaction of hydroxide with epichlorohydrin in the gas phase was studied via *ab initio* calculations. Three mechanisms corresponding to nucleophilic attack at each of the three carbon atoms of epichlorohydrin were considered. Attack at the C1 position was found to be favored over attack at the C3 position at the highest level

of theory. Attack at the C2 position was found to be unlikely. In a subsequent paper, solvent effects upon the reactivity of epichlorohydrin with hydroxide will be reported. It will prove interesting to interpret these results in light of the aforementioned experimental work of McClure *et al.*.[2]

Acknowledgement

It is a pleasure to acknowledge the assistance of Professor Steven R. Kass (University of Minnesota), who read and commented upon an earlier draft of this paper.

REFERENCES

1. (a) *Ullmann's Encyclopedia of Industrial Chemistry* (6th edn), vol. 12. Wiley-VCH: Weinheim, 2003; (b) Kawamura K, Ohta T, Otani G. *Chem. Pharm. Bull.* 1990; **38**: 2092–2096.
2. McClure DE, Arison BH, Baldwin JJ. *J. Am. Chem. Soc.* 1979; **101**: 3666–3668.
3. Ohishi Y, Nakanishi T. *Chem. Pharm. Bull.* 1983; **31**: 3418–3423.
4. Cawley JJ, Onat E. *J. Phys. Org. Chem.* 1994; **7**: 395–398.
5. Whalen DL. *Tetrahedron. Lett.* 1978; **50**: 4973–4976.
6. Politzer P, Laurence PR. *Int. J. Quantum. Chem. Quantum. Biochem. Symp.* 1984; **11**: 155–166.
7. (a) Ditchfield R, Hehre WJ, Pople JA. *J. Chem. Phys.* 1971; **54**: 724–728; (b) Hehre WJ, Ditchfield R, Pople JA. *J. Chem. Phys.* 1972; **56**: 2257–2261; (c) Francl MM, Pietro WJ, Hehre WJ, Binkley JS, Gordon MS, DeFrees DJ, Pople JA. *J. Chem. Phys.* 1982; **77**: 3654–3665.
8. Hariharan PC, Pople JA. *Theor. Chim. Acta* 1973; **28**: 213–222.
9. (a) Clark T, Chandrasekhar J, Spitznagel GW, Schleyer PvR. *J. Comput. Chem.* 1983; **4**: 294–301; (b) Spitznagel GW. *Diplomarbeit*, Erlangen, 1982.
10. (a) Pople JA, Scott AP, Wong MW, Radom L. *Isr. J. Chem.* 1993; **33**: 345–350; (b) Scott AP, Radom L. *J. Phys. Chem.* 1996; **100**: 16502–16513.
11. McQuarrie DA. *Statistical Mechanics*. University Science Books: Sausalito, CA, 2000.
12. Gonzales C, Schlegel HB. *J. Chem. Phys.* 1989; **90**: 2154–2161.
13. Fletcher GD, Rendell AP, Sherwood P. *Mol. Phys.* 1997; **91**: 431–438.
14. (a) Dunning TH Jr. *J. Chem. Phys.* 1989; **90**: 1007–1023; (b) Kendall RA, Dunning TH Jr. *J. Chem. Phys.* 1992; **96**: 6769–6779.
15. Saunders WH Jr. *J. Phys. Org. Chem.* 1994; **7**: 268–271.
16. Schmidt MW, Baldridge KK, Boatz JA, Jensen JH, Koseki S, Matsunaga N, Gordon MS, Nguyen KA, Su S, Windus TL, Elbert ST, Montgomery J, Dupuis M. *J. Comput. Chem.* 1993; **14**: 1347–1363.
17. Wang F, Polavarapu PL. *J. Phys. Chem. A* 2000; **104**: 6189–6196.
18. Hehre WJ, Radom L, Schleyer PvR, Pople JA. *Ab Initio Molecular Orbital Theory*. Wiley: New York, 1986.
19. Cox JD, Wagman DD, Medvedev VA. *CODATA Key Values for Thermodynamics*. Hemisphere: New York, 1984.
20. Bastos M, Nilsson SO, Ribeiro Da Silva MDMC, Ribeiro Da Silva MV. *J. Chem. Thermodyn.* 1988; **20**: 1353–1359.
21. Benson SW. *Thermochemical Kinetics* (2nd edn). Wiley: New York, 1976.
22. Crowder C, Bartmess J. *J. Am. Soc. Mass Spectrom.* 1993; **4**: 723–726.
23. Smith JR, Kim JB, Lineberger WC. *Phys. Rev. A* 1997; **55**: 2036–2043.